

Resonant spin polarization and spin current in a two-dimensional electron gas

Mathias Duckheim and Daniel Loss

Department of Physics and Astronomy, University of Basel, CH-4056 Basel, Switzerland

(Dated: February 6, 2008)

We study the spin polarization and its associated spin-Hall current due to electric-dipole-induced damping of the resonant spin polarization can be strongly reduced by an optimal field configuration that exploits the interference between Rashba and Dresselhaus spin-orbit interaction. This leads to a striking enhancement of the spin susceptibility while the spin-Hall current vanishes at the same time. We give an interpretation of the spin current in geometrical terms which are associated with the trajectories the polarization describes in spin space.

PACS numbers: 73.23.-b, 73.21.Fg, 76.30.-v, 72.25.Rb

The ability to coherently control the spin of charge carriers in semiconductor nanostructures is the main focus of spintronics¹. Band-structure and confinement effects in these systems lead to a strong spin-orbit interaction (SOI) offering the possibility to efficiently access the charge carrier spin via the control of its orbital motion^{2,3,4,5,6,7,8,9,10,11,12,13}.

A versatile and efficient scheme of spin control is electric dipole induced spin resonance (EDSR)^{10,11,14,15,16,17,18,19,20} where electric radio frequency (rf) fields give rise to internal fields coupling to the spin. Choosing an adequate configuration of the electric rf fields and a static magnetic field defining a quantization axis for the spin, arbitrary spin rotations can be realized. This is analogous to standard paramagnetic spin resonance techniques, has the advantage, however, that it can be integrated in gated nanostructures thereby avoiding magnetic rf coils.

In a two-dimensional electron gas (2DEG) with pure Rashba SOI the amount of spin polarization which can be achieved by EDSR is severely limited by disorder¹⁹. Similar limitations are found for pure Dresselhaus SOI. However, if both Dresselhaus and Rashba SOI are present interference between the two SOI mechanisms can occur and qualitatively new behavior emerges, such as anisotropy in spin relaxation^{21,22,23} and transport^{24,25,26}. For spin relaxation this anisotropy is most pronounced if both SOIs have equal strength. In this case, the spin along the $[110]$ direction [see Fig. 1] is conserved^{21,27}, and the associated spin relaxation rates vanish, whereas they become maximal along the perpendicular direction $[\bar{1}\bar{1}0]$. For the driven system considered here we show that similar interference effects occur and that not only the internal rf field but also the EDSR linewidth becomes dependent on the direction of the magnetic field. In a microscopic approach we show then that due to this dependence an optimal configuration exists where the linewidth and the internal field simultaneously become minimal and maximal, resp., and that, as a remarkable consequence, the spin susceptibility gets dramatically enhanced. In other words, this optimal configuration allows one to obtain a high spin polarization with relatively small electric fields and thus making the power consump-

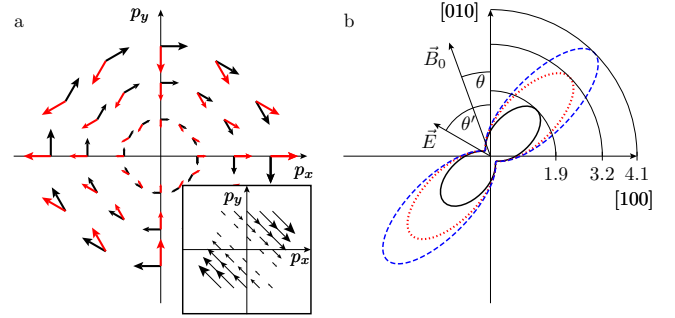


FIG. 1: (color online) a) Momentum dependent magnetic fields induced by Rashba- (black arrows) and Dresselhaus SOI (red arrows) $\Omega_R(\mathbf{p}) = \alpha(p_y, -p_x)$ and $\Omega_D(\mathbf{p}) = \beta(p_x, -p_y)$, respectively. Inset: The sum $\Omega_R + \Omega_D$ for equal strength of the SOI ($\alpha = \beta$) is shown. The interference of the two types of SOI leads to a suppression or enhancement of the spin splitting in certain crystallographic directions. b) Polar plot of the resonance susceptibility $\bar{\chi}^{\text{res}}$ (in arbitrary units) as a function of θ for $\beta = \alpha/2$ and $\omega_L \tau = 1$ (black, solid curve), $\omega_L \tau = 2$ (red, dotted), and $\omega_L \tau = 3$ (blue, dashed). The configuration of the external magnetic and electric field \mathbf{B}_0 and \mathbf{E}_0 is shown. For $\mathbf{B}_0 \parallel \mathbf{E}_0 \parallel [110]$ both SOI contributions add constructively in the direction perpendicular to \mathbf{B}_0 leading to an enlarged Rabi field.

tion for spin polarization minimal.

Due to spin-orbit interaction angular momentum can be transferred between spin and orbital degrees of freedom. This fact leads, in particular, to a dynamical coupling between spin and spin current described by the Heisenberg equation of motion^{19,28,29}. Exploiting this coupling we show that the spin current can be interpreted in geometrical terms: the spin dynamics generated by the rf fields describes an elliptical trajectory. The spin-Hall conductivity can then be expressed entirely in terms of the semi-minor and semi-major axis and the tilt angle of this ellipse. Since the spin dynamics (trajectories) is experimentally accessible, for instance with optical methods^{8,9}, this opens up the possibility for a direct measurement of the spin-Hall current. Finally, we find that for the optimal configuration the spin current vanishes, in stark contrast to the spin polarization which,

as mentioned, becomes maximal.

We consider a non-interacting 2DEG consisting of electrons with mass m and charge e which are subject to a random impurity potential V . We take into account linear SOI $\sum_{ij} \Omega_{ij} p_j \sigma^i$ of the Rashba - and Dresselhaus type where $\sigma^i, i = 1, 2, 3$, are the Pauli matrices and \mathbf{p} is the canonical momentum. Taking the coordinate axes along the $[100], [010], [001]$ crystallographic directions, the internal magnetic field Ω is then given by (cf. Fig.1) $\Omega(\mathbf{p}) = \alpha(p_y, -p_x, 0) + \beta(p_x, -p_y, 0)$ where α and β is the strength of the Rashba and Dresselhaus SOI, respectively. Additionally, the external static magnetic field is given by $\mathbf{B}_0 = B_0 \mathbf{e}_{||}$ with $\mathbf{e}_{||} = (-\sin \theta, \cos \theta, 0)$, and the external electric rf field by $\mathbf{E}(t) = E(t)(-\sin \theta', \cos \theta', 0)$, where θ, θ' are the angles enclosed with the $[010]$ direction. The system is described by the Hamiltonian

$$H = \frac{1}{2m} (\mathbf{p} - e\mathbf{A})^2 + (\Omega(\mathbf{p} - e\mathbf{A}) + \mathbf{b}_0) \cdot \boldsymbol{\sigma} + V, \quad (1)$$

where $\mathbf{A}(t) = -\int^t dt' \mathbf{E}(t')$ is the vector potential associated with \mathbf{E} and $\mathbf{b}_0 = g\mu_B \mathbf{B}_0/2$ with g the electron g -factor and μ_B the Bohr magneton.

Spin polarization. We turn now to the calculation of the spin polarization (magnetization/ μ_B) per unit area, $\mathbf{S}(\omega) = \int_{-\infty}^{\infty} dt e^{i\omega t} \langle \boldsymbol{\sigma}(t) \rangle / 2\pi$, evaluated in linear response to an applied electric field $\mathbf{E}(\omega) = \mathbf{E}_0[\delta(\omega - \omega_0) + \delta(\omega + \omega_0)]/2$ and in the presence of both Rashba and Dresselhaus SOI. Due to the interference between these two SOI mechanisms we need to carefully extend earlier calculations¹⁹, which were restricted to Rashba (Dresselhaus) SOI only, to this new situation. We will then be

able to identify a configuration that allows one to obtain a maximum degree of spin polarization due to this interference.

Working in the linear response regime, $S^i(\omega)$ is obtained from a Kubo formula averaged over the random distribution of impurities in the 2DEG. We evaluate this average with standard diagrammatic techniques assuming the impurities to be short-ranged, isotropic and uniformly distributed. In this case, the impurity average $\overline{V(\mathbf{x})V(\mathbf{x}') \equiv (m\tau)^{-1} \delta(\mathbf{x} - \mathbf{x}')$ is δ -correlated and proportional to the momentum relaxation time τ . We further take the Fermi energy $E_F = p_F^2/2m$ to be the largest energy scale in the problem. Then, to leading order in $1/p_F l$ with $l = p_F/m\tau$ the mean free path, the averaged spin polarization is given by the diffuson diagram, giving rise³⁰ to a correction $\sigma^i \rightarrow \Sigma^i \equiv \Sigma^{ij} \sigma^j$ of the spin vertex (cf. ref.¹⁹) in the Kubo formula. Thus, the spin susceptibility defined by $S^i(\omega) = \chi^{ij}(\omega) E_j(\omega)$ is given by

$$\chi^{ij}(\omega) = \sum_{k=1}^{k=3} 2e\nu\tau \left[\delta^{ik} - \left(1 - \frac{1}{\lambda}\right) \Sigma^{ik} \right] \Omega_{kj}, \quad (2)$$

where $\nu = m/2\pi\hbar^2$ is the two-dimensional density of states and $\lambda(\omega) = 1 - i\omega\tau$.

We evaluate the vertex correction Σ of Eq.(2) for the case of a magnetic field B_0 that is large compared to the internal fields induced by SOI. This regime is characterized by $a_R \equiv \alpha p_F/2b_0 \ll 1$ and $a_D \equiv \beta p_F/2b_0 \ll 1$. The components Σ^{ij} with $i, j = 1, 2, 3$ of the vertex correction are then found to be given by

$$\Sigma = \frac{1}{(\omega_L^2 - \omega^2)\tau^2 + q} \begin{pmatrix} y^2 \frac{\lambda - \cos^2(\theta)}{\lambda - 1} + \lambda(\lambda - 1) + q_{11} & \frac{-y^2}{2(\lambda - 1)} \sin(2\theta) + q_{12} & y \cos(\theta) + q_{13} \\ \frac{-y^2}{2(\lambda - 1)} \sin(2\theta) + q_{12} & y^2 \frac{\lambda - \sin^2(\theta)}{\lambda - 1} + \lambda(\lambda - 1) + q_{22} & y \sin(\theta) + q_{23} \\ -y \cos(\theta) - q_{13} & -y \sin(\theta) - q_{23} & y^2 + \lambda(\lambda - 1) + q_{33} \end{pmatrix}, \quad (3)$$

where $y = 2b_0\tau/\hbar = \omega_L\tau$. Here, the functions q_{ij} and q are second order in a_R and a_D , and depend on the frequency ω , the Larmor frequency ω_L , and the angle θ ³⁶. In the EDSR system, Pauli paramagnetism gives rise to a constant equilibrium polarization $\mathbf{S}_{\text{eq}} = \nu\hbar\omega_L \mathbf{e}_{||}$ along \mathbf{B}_0 which is independent of the electric field. The polarization dynamically generated by $\mathbf{E}(\omega)$, however, depends on the amplitude of the oscillating internal field perpendicular to \mathbf{B}_0 . It is thus instructive to consider the longitudinal (along $\mathbf{B}_0 || \mathbf{e}_{||}$) and the transverse (along $\mathbf{e}_{\perp} \equiv \mathbf{e}_{||} \times \mathbf{e}_3$ and \mathbf{e}_3) polarization components given by $S'^2 = \mathbf{e}_{||} \cdot \mathbf{S}$ and $S'^1 = \mathbf{e}_{\perp} \cdot \mathbf{S}$, $S'^3 = S^3$, resp.

As a result, we find the polarization $S'^i(\omega) = \bar{\chi}^i(\omega, \theta') E(\omega)$ in terms of the transformed susceptibility $\bar{\chi}$. To lowest order in a_R, a_D only the transverse compo-

nents ($i = 1, 3$) are finite. They are given by

$$\bar{\chi}^i(\omega, \theta') = S_{\text{eq}} l(\omega) [\alpha \cos(\theta' - \theta) - \beta \sin(\theta' + \theta)] \times w_i \left(\frac{1}{\omega_L - \omega + \delta\omega - i\Gamma} + \frac{1}{\omega_L + \omega - \delta\omega + i\Gamma} \right), \quad (4)$$

where $w_1 = 1$ for the in-plane ($i = 1$) and $w_3 = -i\omega/\omega_L$ for the out-of-plane component ($i = 3$), and $l(\omega) = e\tau/\hbar(1 - i\omega\tau)$ is proportional to the Drude conductivity³⁷.

Close to resonance the scattering from disorder leads to a renormalization of the magnetic field dependence.

The resonance is shifted by a term

$$\begin{aligned} \delta\omega &= \text{Re } q(\omega = \omega_L)/2\omega_L\tau^2 \\ &= \frac{p_F^2\tau}{\hbar^2}[\alpha^2 + \beta^2 - 2\beta\alpha\sin(2\theta)]\frac{\omega_L\tau}{1 + (\omega_L\tau)^2}, \end{aligned} \quad (5)$$

corresponding to an effective g-factor which depends both on the amplitude and the orientation of the magnetic field. The linewidth Γ of the resonance peak is given by

$$\begin{aligned} \Gamma &= -\text{Im } q(\omega = \omega_L)/2\omega_L\tau^2 = 2p_F^2\tau/\hbar^2 \\ &\times \left[(\alpha^2 + \beta^2 + 2\alpha\beta\sin(2\theta)) + \frac{(\alpha^2 + \beta^2) - 2\alpha\beta\sin(2\theta)}{2[1 + (\omega_L\tau)^2]} \right]. \end{aligned} \quad (6)$$

Note that in Γ the Rashba and Dresselhaus SOI do not simply add up but can interfere with each other, enabling a strong enhancement of the susceptibility as we will see next. In Fig. 1 we plot the spin susceptibility at resonance, $\bar{\chi}^{\text{res}} \propto [\cos(\theta' - \theta) - \sin(\theta' + \theta)\rho]/\Gamma$ for the case $\rho = \beta/\alpha = 0.5$ measured in²⁵. The angle θ' has been tuned to maximize $\bar{\chi}^{\text{res}}$ which displays a pronounced dependence on the magnetic field direction. In Eq. (6) we note that Γ scales with the mean square fluctuations of the internal magnetic fields $\langle (\mathbf{e}_{\parallel} \cdot \mathbf{\Omega}(p_F\hat{\mathbf{n}}))^2 \rangle_{\hat{\mathbf{n}}}$ and $\langle (\mathbf{e}_{\perp} \cdot \mathbf{\Omega}(p_F\hat{\mathbf{n}}))^2 \rangle_{\hat{\mathbf{n}}}$, where $\langle \cdot \rangle_{\hat{\mathbf{n}}}$ denotes a uniform average over all (in-plane) directions $\hat{\mathbf{n}}$. Comparison with a simple model^{31,32} of spin relaxation (Bloch equation) shows that the first term in Eq. (6) comes from pure dephasing, i.e. from disorder induced fluctuations of the internal fields along \mathbf{B}_0 , while the second term is due to fluctuations along \mathbf{e}_{\perp} . Choosing a configuration with $\theta = \theta' = -\pi/4$ and tuning the SOI strengths to $\alpha = \beta$ the first term vanishes while the second is subject to narrowing due to the magnetic field. The width becomes $\Gamma_{\text{DP}}/[1 + (\omega\tau)^2]$ where $\Gamma_{\text{DP}} = 2(\alpha p_F)^2\tau/\hbar^2$ is the D'yakonov - Perel spin relaxation rate for Rashba SOI. Increasing the frequency such that (at resonance) $\omega_L\tau = \omega\tau \gg 1$ will lead to an increase of the inverse width Γ^{-1} and, hence, of the susceptibility at resonance, given by

$$|\bar{\chi}_{\alpha=\beta}^{\text{res}}| = S_{\text{eq}} \frac{e\alpha\tau}{\hbar\Gamma_{\text{DP}}} \sqrt{1 + (\omega_L\tau)^2}. \quad (7)$$

For comparison, we find the ratio to the resonance susceptibility $\bar{\chi}_{\beta=0}^{\text{res}}$ in the pure Rashba case as $|\bar{\chi}_{\alpha=\beta}^{\text{res}}/\bar{\chi}_{\beta=0}^{\text{res}}| = (1 + y^2)[1 + 1/(2(1 + y^2))]$ growing quadratically with $y = \omega_L\tau$. Thus, the spin polarization can be substantially enhanced by tuning the SOIs to equal strengths and by increasing the magnetic field. Finally, the range of validity for the linear response regime can be estimated as follows. Assuming full polarization ($|S'_{\alpha=\beta}|/S_{\text{eq}} \approx 1$) and parameters for a GaAs 2DEG⁹ with spin-orbit splitting $\Delta_{\text{SO}} = \alpha p_F = 60 \mu\text{eV}$, Fermi wavelength $\lambda_F = 180 \text{ nm}$ and $\omega_L\tau = 10$, we find from Eq. (7) that the linear response is valid for electric fields with amplitudes up to $E_0 = 2\pi\Delta_{\text{SO}}/\lambda_F\omega_L\tau \approx 200 \text{ eVm}^{-1}$.

Polarization and Spin current. We consider the spin current defined by $\mathbf{I}^3 = \langle \{\sigma^3, \mathbf{v}\} \rangle / 2$. Using the Heisenberg equation of motion the spin current components $I_{x'}^3$

and $I_{y'}^3$, along \mathbf{e}_{\perp} and \mathbf{e}_{\parallel} can be expressed in terms of the polarization at frequency ω as

$$\begin{aligned} \begin{pmatrix} I_{x'}^3 \\ I_{y'}^3 \end{pmatrix} &= \frac{\hbar}{2m(\alpha^2 - \beta^2)} \\ &\times \begin{pmatrix} [\alpha - \beta\sin(2\theta)](i\omega S'^1 + \omega_L S'^3) - i\omega\beta\cos(2\theta)S'^2 \\ (\alpha + \beta\sin(2\theta))i\omega S'^2 - \beta\cos(2\theta)(i\omega S'^1 + \omega_L S'^3) \end{pmatrix}. \end{aligned} \quad (8)$$

We consider the configuration $\theta = \theta' = -\pi/4$ such that the SOI induced internal rf field is perpendicular to \mathbf{B}_0 and the longitudinal component $S'^2(t) = S_{\text{eq}}$ is not altered in linear response in E . Note that in this case Eq.(8) simplifies such that $I_{x'}^3 = \hbar(i\omega S'^1 + \omega_L S'^3)/(2m(\alpha - \beta))$. This relation differs from the naive model of an average spin-orbit field equating the internal field $\mathbf{\Omega}(\mathbf{p}(t))$ with its average $\mathbf{\Omega}(\langle \mathbf{p} \rangle(t))$. Contrary to Eq.(8), we then find $i\omega S'^1 + \omega_L S'^3 = \Gamma^1 S'^1$ where Γ^1 is a phenomenological transverse relaxation rate. Discrepancies to the model of an averaged spin-orbit field occur similarly for other effects such as the generation of an out-of plane polarization³³ and Zitterbewegung³⁴.

We proceed by evaluating the spin-Hall current $I_{x'}^3$ in terms of the vertex correction Eq.(3) which was obtained in the diagrammatic approach and is valid up to second order in a_R, a_D . The linear combination $i\omega S'^1 + \omega_L S'^3$ cancels in lowest order (cf. Eq.(4)) such that $I_{x'}^3$ is given by the second order terms q_{ij}, q . From Eq.(2) and Eq.(8) we find the spin-Hall conductivity, defined as $\sigma_{x'y'}^{3,\text{res}} = \hbar I_{x'}^3/2E(\omega)$, to be given by

$$\sigma_{x'y'}^{3,\text{res}} = \frac{e}{4\pi} \frac{i\omega_L\tau(\alpha^2 - \beta^2)}{(3\alpha^2 - 2\alpha\beta + 3\beta^2) - i2\omega_L\tau(\alpha - \beta)^2}. \quad (9)$$

Remarkably, for high frequencies $\omega_L\tau(\alpha - \beta)^2 \gg (\alpha + \beta)^2$ and $\alpha \neq \beta$ Eq.(9) reaches the universal limit $\sigma_{x'y'}^{3,\text{res}} = |e|/8\pi \times (\alpha + \beta)/(\alpha - \beta)$ (independent of the disorder details). This limit depends only on the ratio α/β of the strengths of the SOIs, but not on their absolute values, and agrees with the clean limit found in³⁵ for $\beta = 0$. Indeed, for the condition $\omega_L\tau \gg 1$ ($\omega_L = \omega$), many cycles of the electric rf field pass through between subsequent scattering events such that the system effectively behaves as ballistic. This regime can be exploited to achieve high spin polarizations as described above.

Moreover, the singularity in Eq.(8) for $\alpha = \beta$ is removed in Eq.(9) up to the accuracy $\mathcal{O}(a_R^2, a_D^2, a_D a_R)$ considered here and we find that $\sigma_{x'y'}^{3,\text{res}}$ vanishes in the configuration where $\bar{\chi}$ is maximal, i.e. for $\alpha = \beta$ and $\theta = \theta' = -\pi/4$.

We turn now to a geometrical interpretation of the spin Hall current relating it to the trajectories $\mathcal{S} = \{(S'^1(t), S'^3(t)) | t \in \mathbb{R}\}$ followed by the tip of the polarization vector. For an applied electric field $\mathbf{E}(\omega) = E_0\mathbf{e}_{\parallel}[\delta(\omega - \omega_0) + \delta(\omega + \omega_0)]/2$ with frequency ω_0 this trajectory is given by the polarization (as a function of time)

$$\begin{pmatrix} S'^1(t) \\ S'^3(t) \end{pmatrix} = \Lambda(\omega_0) \begin{pmatrix} \cos \omega_0 t \\ \sin \omega_0 t \end{pmatrix} \quad (10)$$

with the matrix

$$\Lambda(\omega_0) = E_0 \begin{pmatrix} \text{Re}\bar{\chi}^1(\omega_0) & -\text{Im}\bar{\chi}^1(\omega_0) \\ \text{Re}\bar{\chi}^3(\omega_0) & -\text{Im}\bar{\chi}^3(\omega_0) \end{pmatrix} \quad (11)$$

containing the Fourier components $\bar{\chi}^{1,3}(\omega)$ of the susceptibility evaluated at $\omega = \omega_0$. Eq. (10) constitutes a quadratic form for the trajectory given by $\mathbf{S} = \{(S'^1, S'^3) | \mathbf{S}'^t \cdot \Lambda_2 \mathbf{S}' = 1\}$ with real, positive eigenvalues $\lambda_{1,2}$ (say $\lambda_1 < \lambda_2$) of the defining matrix $\Lambda_2 = (\Lambda^{-1})^t \Lambda^{-1}$. Thus, \mathbf{S} is of elliptic shape with semi-major and semi-minor axis $a = 1/\sqrt{\lambda_1}$ and $b = 1/\sqrt{\lambda_2}$, resp. We can further determine the angle δ enclosed by the semi-major axis of \mathbf{S} and the S'^1 direction since the matrix Λ_2 is diagonalized by a rotation δ around S'^2 . The polarization of Eq. (10) can thus be written as

$$\begin{pmatrix} S'^1(t) \\ S'^3(t) \end{pmatrix} = \begin{pmatrix} \cos \delta & -\sin \delta \\ \sin \delta & \cos \delta \end{pmatrix} \begin{pmatrix} a \cos(\omega_0 t + \varphi) \\ b \sin(\omega_0 t + \varphi) \end{pmatrix}. \quad (12)$$

Here, φ is a phase shift between the electric field and the polarization. From Eqs. (10) and (12), we can relate the real and imaginary part of the susceptibilities $\bar{\chi}^1$ and $\bar{\chi}^3$ to the parameters a, b, φ , and δ . In particular, we obtain the spin Hall current (Eq.(8)) at resonance ($\omega_L = \omega$) as

$$I_{x'}^3(\omega) = \frac{\hbar E(\omega) e^{i(\varphi-\delta)}}{2m(\alpha - \beta)E_0} i\omega_L(a - b). \quad (13)$$

Eq. (13) provides a remarkable interpretation of the spin Hall current in terms of the geometric properties of the orbit \mathbf{S} . The component $I_{x'}^3$ is given by a complex phase depending on the rotation angle δ and the difference between the semi-minor and semi-major axis $a - b$. In the linear response regime, the spin Hall current characterizes the deviation from a circular orbit with $a = b$ to an elliptic shape (with $a \neq b$). Therefore, $I_{x'}^3$ becomes accessible in terms of simple geometric properties of \mathbf{S} in experiments capable of resolving individual polarization components.

In conclusion, we predict a substantially enhanced spin polarization due to interference effects of Rashba and Dresselhaus SOI. The spin Hall current associated with this polarization can be interpreted in terms of the trajectory in spin space and vanishes if the polarization is maximal.

We thank O. Chalaev, D. Bulaev, J. Lehmann, and H.-A. Engel for helpful discussions. We acknowledge financial support from the Swiss NF, NCCR Nanoscience Basel, and the ONR.

APPENDIX A: FUNCTIONS

For $\theta = -\pi/4$, $\omega = \omega_L$, and $\rho = \beta/\alpha$ the functions q and q_{ij} are given by

$$q_{11} = \frac{-2a_R^2(\lambda - 1)^2\lambda}{(1 - 2\lambda)^2} \quad (A1)$$

$$\begin{aligned} & \times [1 + 6\lambda^2(\rho - 1)^2 + (\rho - 8)\rho - 4\lambda(1 + (\rho - 5)\rho)] , \\ q_{12} &= \frac{-2a_R^2(\lambda - 1)^2}{(1 - 2\lambda)^2} \quad (A2) \\ & \times [2\lambda^3(\rho - 1)^2 + 4\lambda^2\rho + (1 + \rho)^2 - \lambda(3 + \rho(4 + 3\rho))] , \end{aligned}$$

$$\begin{aligned} q_{13} &= \frac{i\sqrt{2}a_R^2(\lambda - 1)^2}{(1 - 2\lambda)^2} [1 + 4\lambda^3(\rho - 1)^2 + \rho(6 + \rho) \quad (A3) \\ & - 4\lambda^2(1 + (\rho - 4)\rho) - 2\lambda(1 + \rho(8 + \rho))] , \end{aligned}$$

$$\begin{aligned} q_{33} &= \frac{-2a_R^2(\lambda - 1)^2}{\lambda(1 - 2\lambda)^2} [4\lambda^4(\rho - 1)^2 - 12\lambda^2\rho \quad (A4) \\ & - (1 + \rho)^2 + 3\lambda(1 + \rho)^2 - 4\lambda^3(1 + (\rho - 4)\rho)] , \end{aligned}$$

and $q_{22} = q_{11}$ and $q_{23} = q_{13}$.

-
- ¹ D. D. Awschalom, D. Loss, and N. Samarth, eds., *Semiconductor Spintronics and Quantum Computation* (Springer, Berlin, 2002).
² V. M. Edelstein, *Solid State Comm.* **73**, 233 (1990).
³ Y. Kato, R. C. Myers, D. C. Driscoll, A. C. Gossard, J. Levy, and D. D. Awschalom, *Science* **299**, 1201 (2003).
⁴ E. I. Rashba and A. L. Efros, *Phys. Rev. Lett.* **91**, 126405 (2003).
⁵ M. I. D'yakonov and M. I. Perel, *JETP Lett.* **13**, 467 (1971).
⁶ S. Murakami, N. Nagaosa, and S. C. Zhang, *Science* **301**, 1348 (2004).
⁷ J. Sinova, D. Culcer, Q. Niu, N. A. Sinitsyn, T. Jungwirth, and A. H. MacDonald, *Phys. Rev. Lett.* **92**, 126603 (2004).
⁸ Y. K. Kato, R. C. Myers, A. C. Gossard, and D. D.

- Awschalom, *Science* **306**, 1910 (2004).
⁹ V. Sih, R. C. Myers, Y. K. Kato, W. H. Lau, A. C. Gossard, and D. D. Awschalom, *Nature Physics* **1**, 31 (2005).
¹⁰ D. V. Bulaev and D. Loss, *Phys. Rev. Lett.* **98**, 097202 (2007).
¹¹ V. N. Golovach, M. Borhani, and D. Loss, *Phys. Rev. B* **74**, 165319 (2006).
¹² M. Trif, V. N. Golovach, and D. Loss, *Phys. Rev. B* **75**, 085307 (2007).
¹³ A. Shnirman and I. Martin, *Europhys. Lett.* **78**, 27001 (2007).
¹⁴ R. L. Bell, *Phys. Rev. Lett.* **9**, 52 (1962).
¹⁵ M. Dobrowolska, A. Witowski, J. K. Furdyna, T. Ichiguchi, H. D. Drew, and P. A. Wolff, *Phys. Rev. B* **29**, 6652 (1984).
¹⁶ E. I. Rashba and A. L. Efros, *App. Phys. Lett.* **83**, 5295

- (2003).
- ¹⁷ M. Schulte, J. G. S. Lok, G. Denninger, and W. Dietsche, Phys. Rev. Lett. **94**, 137601 (2005).
 - ¹⁸ Y. K. Kato, R. C. Myers, A. C. Gossard, and D. D. Awschalom, Nature **427**, 50 (2004).
 - ¹⁹ M. Duckheim and D. Loss, Nature Physics **2**, 195 (2006).
 - ²⁰ Z. Wilamowski, H. Malissa, F. Schäffler, and W. Jantsch, Phys. Rev. Lett. **98**, 187203 (2007).
 - ²¹ N. S. Averkiev, L. E. Golub, and M. Willander, J. Phys.: Condens. Matter **14**, R271R283 (2002).
 - ²² V. N. Golovach, A. Khaetskii, and D. Loss, Phys. Rev. Lett. **93**, 016601 (2004).
 - ²³ Y. Li and Y.-Q. Li (2006), cond-mat/0610694.
 - ²⁴ J. Schliemann and D. Loss, Phys. Rev. B **68**, 165311 (2003).
 - ²⁵ S. D. Ganichev, V. V. Bel'kov, L. E. Golub, E. L. Ivchenko, P. Schneider, S. Giglberger, J. Eroms, J. D. Boeck, G. Borghs, W. Wegscheider, et al., Phys. Rev. Lett. **92**, 256601 (2004).
 - ²⁶ M. Trushin and J. Schliemann, Phys. Rev. B **75**, 155323 (2007).
 - ²⁷ J. Schliemann, J. C. Egues, and D. Loss, Phys. Rev. Lett. **90**, 146801 (2003).
 - ²⁸ S. I. Erlingsson, J. Schliemann, and D. Loss, Phys. Rev. B **71**, 035319 (2005).
 - ²⁹ O. Chalaev and D. Loss, Phys. Rev. B **71**, 245318 (2005).
 - ³⁰ J. Rammer, *Quantum Transport Theory* (Perseus Books, Reading, Massachusetts, 1998).
 - ³¹ F. Bloch, Phys. Rev. **105**, 1206 (1957).
 - ³² C. Tahan and R. Joynt, Phys. Rev. B **71**, 075315 (2005).
 - ³³ H.-A. Engel, E. I. Rashba, and B. I. Halperin, Phys. Rev. Lett. **98**, 036602 (2007).
 - ³⁴ J. Schliemann, D. Loss, and R. M. Westervelt, Phys. Rev. Lett. **94**, 206801 (2005).
 - ³⁵ E. G. Mishchenko, A. V. Shytov, and B. I. Halperin, Phys. Rev. Lett. **93**, 226602 (2004).
 - ³⁶ The q_{ij} and q are too lengthy to be written down here. In the following, only $\text{Im } q$, $\text{Re } q$ and the linear combination $\sqrt{2}(q_{13}-q_{23})y+(q_{11}-2q_{12}+q_{22})(\lambda-1)-2\lambda q$ are relevant for the linewidth and the spin-Hall conductivity, resp., which are explicitly given below in Eqs.(6) and (9).
 - ³⁷ From Eq.(4) we can identify the component of the internal rf field $b_1(\omega)$ (which effectively drives the spin dynamics) in terms of the electrically induced momentum drift $\langle \mathbf{p} \rangle(\omega) = \hbar l(\omega) \mathbf{E}(\omega)$. We find that $b_1(\omega) = \mathbf{e}_\perp \cdot \boldsymbol{\Omega}(\langle \mathbf{p} \rangle(\omega))$ is given by the projection of the internal rf field (induced by $\langle \mathbf{p} \rangle(\omega)$) on the transverse direction \mathbf{e}_\perp . Note that due to disorder scattering the Fourier transform $\langle \mathbf{p} \rangle(t)$ and $b_1(t)$ are phase-lagged with respect to $\mathbf{E}(t)$.